Quaternary Science Reviews 363 (2025) 109429

Contents lists available at ScienceDirect

Quaternary Science Reviews

journal homepage: www.elsevier.com/locate/quascirev

Regional climatic dynamics and cultural divergence in glacial western Europe

Olivier Cartapanis [a,*], Edouard Bard [a], Suzanne A.G. Leroy [b,c], Manuel Chevalier [d], Damien Flas [b,e], Thibaut Devièse [a]

[a] Aix-Marseille University, CNRS, IRD, Collège de France, INRAE, CEREGE, UMR7330, Avenue Louis Philibert, 13545, Aix-en-Provence, France
[b] Aix Marseille University, CNRS, Ministère de la Culture, LAMPEA, UMR 7269, 5 rue du Château de l'Horloge, 13094, Aix-en-Provence, France
[c] School of Environmental Sciences, University of Liverpool, Lancashire, Liverpool, L69 7ZT, UK
[d] Institute of Geosciences, Sect. Meteorology, Rheinische Friedrich-Wilhelms-Universität Bonn, Auf dem Hügel 20, 53121, Bonn, Germany
[e] Service de Préhistoire, Université de Liège, 7 Place du 20 Août, 4000, Liège, Belgium

ARTICLE INFO

Handling Editor: Dr I Hendy

Keywords:
Western Europe climate
Millenial-scale variability
Last glacial period
Palaeotemperature proxies
Pollen assemblages
Climate forcing and feedback
Châtelperronian and Uluzzian techno-complexes

ABSTRACT

Western European climate during the Last Glacial period (50–20 ka BP) was shaped by complex interactions between oceanic and terrestrial conditions, modulated by both orbital and millennial-scale forcings. This study integrates 75 marine and terrestrial palaeoenvironmental records to reconstruct spatiotemporal climate variability across Europe and the Mediterranean region. Sea surface temperature (SST) records reveal a pronounced latitudinal gradient, with strong cooling at high latitudes and relative SST stability at mid-latitudes on multi-millennial timescales, which likely moderated western European climate. Pollen-based vegetation records, in contrast, show a steep longitudinal trend, with intensified environmental shifts southeast of the Alps, where oceanic moderation was limited. On millennial timescales, Dansgaard-Oeschger cycles and Heinrich stadials imprinted distinct signatures on SST and vegetation, especially near the Atlantic margin, linked to disruptions in the Atlantic Meridional Overturning Circulation. These findings highlight the differentiated sensitivity of oceanic and terrestrial conditions to climate drivers and the climatic role of geographic barriers such as the Alps. The resulting spatial heterogeneity likely influenced human cultural trajectories, with stable long-term conditions but strong Heinrich stadial near the Atlantic coinciding with the emergence of the Châtelperronian industry, while more pronounced climatic long-term trend in southeastern Europe paralleled the development of the Uluzzian complex. This integrated palaeoenvironmental framework provides critical context for interpreting Late Pleistocene human adaptation and innovation in Europe.

1. Introduction

Understanding how climate variability shaped environmental conditions is essential not only for reconstructing past ecosystems but also for evaluating the challenges prehistoric human populations faced—particularly during periods of cultural and demographic changes such as the Middle to Upper Palaeolithic transition. Climatic shifts likely played a central role in influencing human dispersals, cultural innovations, and adaptive strategies across Europe during the Late Pleistocene.

At the global scale, climate during the last glacial period was primarily driven by changes in summer insolation at the critical latitude of 65°N, which modulated ice sheet volume, notably the expansion and retreat of the Eurasian ice cap (Fig. 1). These changes, in turn, affected Earth's radiative budget through albedo and influenced the carbon cycle via shifts in ocean circulation and biological productivity, driving fluctuations in atmospheric pCO_2 and global temperatures.

Superimposed on these long-term trends were shorter-term climatic oscillations. Variations in solar energy by latitude and season (Berger, 1981; Loutre et al., 2004), along with changes in vegetation, sea ice, and atmospheric-oceanic circulation, led to complex regional patterns over multi-millennial timescales (≥10 ka). Greenland ice core records reveal a millennial-scale sequence of abrupt warm (interstadials) and cold phases (stadials) with saw-tooth-like pattern (Fig. 2) known as Dansgaard-Oeschger (DO) cycles. Some stadials were accompanied by massive iceberg discharges affecting large portion of the North Atlantic

* Corresponding author.
E-mail address: cartapanis@cerege.fr (O. Cartapanis).

https://doi.org/10.1016/j.quascirev.2025.109429
Received 22 January 2025; Received in revised form 16 May 2025; Accepted 16 May 2025
Available online 31 May 2025

north of 40°N (Heinrich stadials; Heinrich, 1988; Bond et al., 1992; Bard et al., 2000; Hemming, 2004; van Kreveld et al., 2000). These events disrupted the Atlantic Meridional Overturning Circulation (AMOC), altering global heat redistribution and the carbon cycle (McManus et al., 2004; Henry et al., 2016).

These external forcings and internal feedbacks operated across multiple spatial and temporal scales and interacted with each other, contributing to the modulation of global climatic trends at diverse temporal and spatial scales. In other words, regional environmental responses to these climate drivers varied considerably. For example, precession influenced vegetation dynamics south of 40°N, while obliquity had greater effects at higher latitudes (Fletcher and Sánchez Goñi, 2008; Fletcher et al., 2010). The interplay between orbital parameters, ice sheet extent, greenhouse gas concentrations, and oceanic conditions created spatial and temporal variability in climate expression, particularly during Heinrich stadials (Sánchez Goñi et al., 2021; Fourcade et al., 2024). These dynamics underscore the value of integrating terrestrial and marine palaeoenvironmental records to reconstruct environmental conditions at scales relevant to human lifeways.

However, the precise timing, geographic extent, and mechanisms by which global trends translated into local environmental changes remain insufficiently understood. This matter is particularly important during the 50–20 ka BP interval—a critical time window encompassing the Middle and Upper Palaeolithic transition and the emergence of techno-complexes such as the Châtelperronian and Uluzzian in different regions (Higham et al., 2024; Charton et al., 2025; Marciani et al., 2025). This period is one of the best documented in palaeoclimatic research, owing to a wealth of archives and relatively robust radiocarbon chronologies.

Despite the abundance of marine sea surface temperature (SST) records from the North Atlantic and Mediterranean regions, inland responses remain less well characterized. Oceanic climate strongly influences coastal zones (Dommenget, 2009; Sung et al., 2023), but interior regions diverge due to contrasted sensitivity to insolation, topography, atmospheric circulation, and vegetation feedbacks (Cartapanis et al., 2022). Among terrestrial proxies, pollen records stand out for their spatial coverage and sensitivity to regional environmental conditions. When interpreted through the lens of biomes or megabiomes (Prentice et al., 1992; Fletcher et al., 2010; Sánchez Goñi et al., 2017), they offer powerful insights into past climate constraints on vegetation.

In this study, we integrate SST and pollen-based records across the Euro-Mediterranean region to assess environmental variability between 50 and 20 ka BP. By harmonizing chronologies, calibrating SST proxies, and applying consistent biome classifications, we identify spatiotemporal palaeoclimatic and palaeoenvironmental patterns and investigate how different climatic forcings—orbital, oceanic, and atmospheric—may have influenced prehistoric populations. Special attention is given to the implications of these changes for the emergence and spread of Châtelperronian and Uluzzian techno-complexes.

2. Material and methods

2.1. Data collection strategy

We gathered 75 palaeoclimatic proxy records from 53 archives (32 oceanic sediment cores and 21 continental archives, Fig. 1) to characterize the main climatic trends across western Europe and the border of the Mediterranean basin during the late glacial period (Fig. 1). These datasets were downloaded from online data repositories, i.e. PANGAEA (Felden et al., 2023), NOAA (https://www.ncei.noaa.gov/access/paleo-search/), NEOTOMA (Williams et al., 2018) and individual studies or compilations (Sánchez Goñi et al., 2017; Waelbroeck et al., 2019; Pedro et al., 2022). The 32 marine archives analyzed are distributed between 67 and 36°N, and 47°W and 36°E, with a higher density in coastal regions and along the Iberian margin (Fig. 1; see also Supplementary Table 1). In contrast, the 21 terrestrial archives are distributed between 50 and 31°N, and 6°W and 35°E. This results in a significant difference in the continental archive distribution with more records in the southwestern part of the study domain compared to the marine archives. Consequently, this bias affects the spatial distribution of pollen records relative to SST proxies.

2.2. Chronological constraints strategy

For most of the selected archives, chronological constraints were obtained from the most recent publication on each archive or from proxy compilations (Sánchez Goñi et al., 2017; Waelbroeck et al., 2019; Li et al., 2022). The ^{14}C dates were re-calibrated with the most recent calibration curves to produce a framework with consistent chronological uncertainties. Age models were created using the Undatable software (Lougheed and Obrochta, 2019), an age-depth modelling technique that

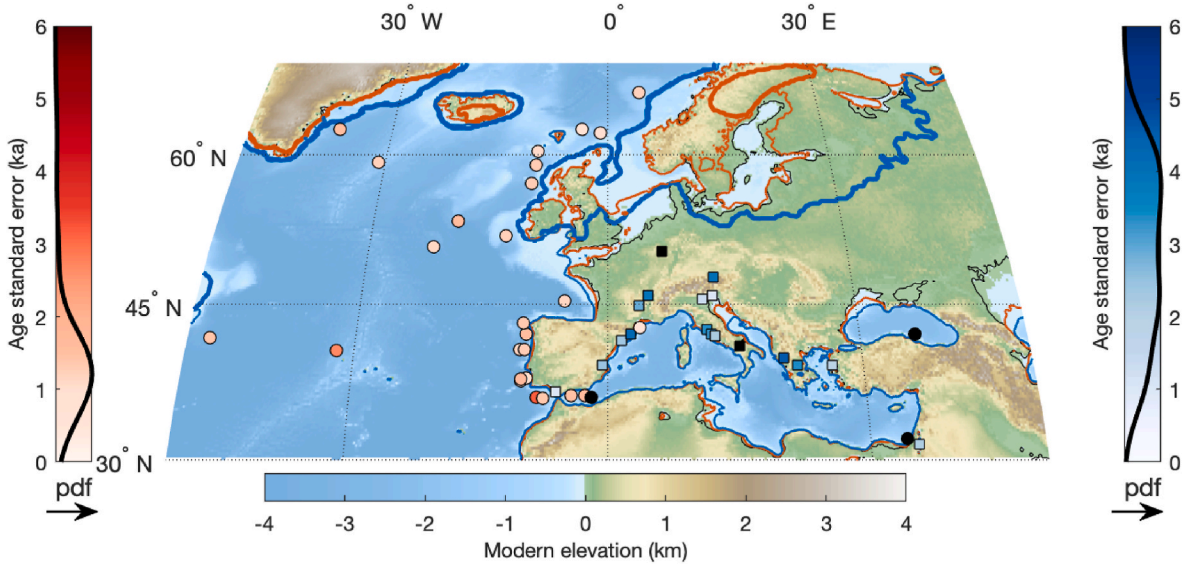

Fig. 1. Mean standard error of age model for continental (square, blue scale) and marine (dots, red scale) archives for the 50-20 ka period. Probability density function of mean standard error for marine and terrestrial archives are also displayed in their respective color bar. Black filling indicates archives for which the age model was reproduced from the original publication. Red and blue thick lines show ice sheet extension at 50 ka and LGM respectively (Gowan et al., 2021). The thin red and blue lines represent coastlines at 50 and 20 ka respectively (Gowan et al., 2021).

uses Bayesian radiocarbon calibration (Lougheed and Obrochta, 2016).

The ^{14}C ages from marine settings were calibrated using the Marine20 calibration curve (Heaton et al., 2023b). Local reservoir ages for the Holocene were computed following Reimer and Reimer (2001) (http://calib.org/marine/; last accessed 16 August 2023). Before the Holocene (11,500 cal BP), reservoir ages depend on oceanic circulation and were inferred following Heaton et al. (2023a,b) using glacial state scenario (GS) and the more extreme cold stadial (CS) scenario with reduced AMOC during Heinrich stadials. We used the IntCal20 calibration curve in terrestrial settings (Reimer et al., 2020).

Additional non–radiocarbon tie points used for building chronologies were retrieved from the literature and defined by matching proxy records with Greenland ice core records using the Greenland Ice Core Chronology 2005 timescale (Andersen et al., 2006; Svensson et al., 2006, 2008) with the exception of a few tephra and U/Th dates. Due to the complexity of the archive stratigraphy (such as inclusion of varve counting or composite records), we reproduced the age models of seven records directly from their reference publication. Age model construction details are provided in the supplementary information.

2.3. Sea surface temperature records

The foraminiferal-based SST reconstructions compiled here (23 records, see Supplementary Fig. S6) were calibrated to summer temperature (Pedro et al., 2022) and developed using the maximum likelihood technique (ter Braak and van Dame, 1989). UK'_{37} datasets (8 records) were calibrated to mean annual Sea Surface Temperatures using BAYSPLINE, a Bayesian calibration tool for alkenone palaeothermometer (Tierney and Tingley, 2018). Bayesian spatially varying calibration was used to infer mean annual SST values from TEX_{86} (Tierney and Tingley, 2014, 5 records). The calibration of sea surface temperature proxy records based on the Mg/Ca ratio in microfossils (4 records) varies amongst species and locations and depends on the cleaning method. They were consequently not modified from the original publication. Similarly, the calibration of records based on dinocysts assemblages (2 records) was not modified from the original publications. Bayesian calibration and alternative calibration for UK'_{37} and TEX_{86} (Conte et al., 2006; Kim et al., 2008) are provided in the supplementary data.

2.4. Pollen records

A total of 33 pollen assemblage records were compiled from published datasets or provided directly by the authors. Most datasets consisted of raw pollen counts; however, two were available only as percentages of total counts, and two others (Les Echets and Lac du Bouchet) were digitized from published figures in the ACER database (Sánchez Goñi et al., 2017). To enable continental-scale site comparisons, taxa were classified using the seven mega-biome classification scheme defined by Fletcher et al. (2010), with the addition of an eighth category, 'Tropical elements', and several supplementary taxa in each group (Table 1). In marine settings, *Pinus* was excluded from percentage calculations due to its frequent over-representation caused by transport processes (Heusser and Balsam, 1977; Naughton et al., 2007).

We then calculated the ratio of the combined warm temperate forest and temperate forest megabiomes (Tf) to the sum of non-temperate forest taxa (nTf) as a proxy for temperate forest coverage (Tf/nTf; Supplementary Fig. S6). Because this ratio is derived from compositional data, it exhibits a log-normal distribution and is heavily skewed toward higher values, making it unsuitable for conventional Gaussian statistical

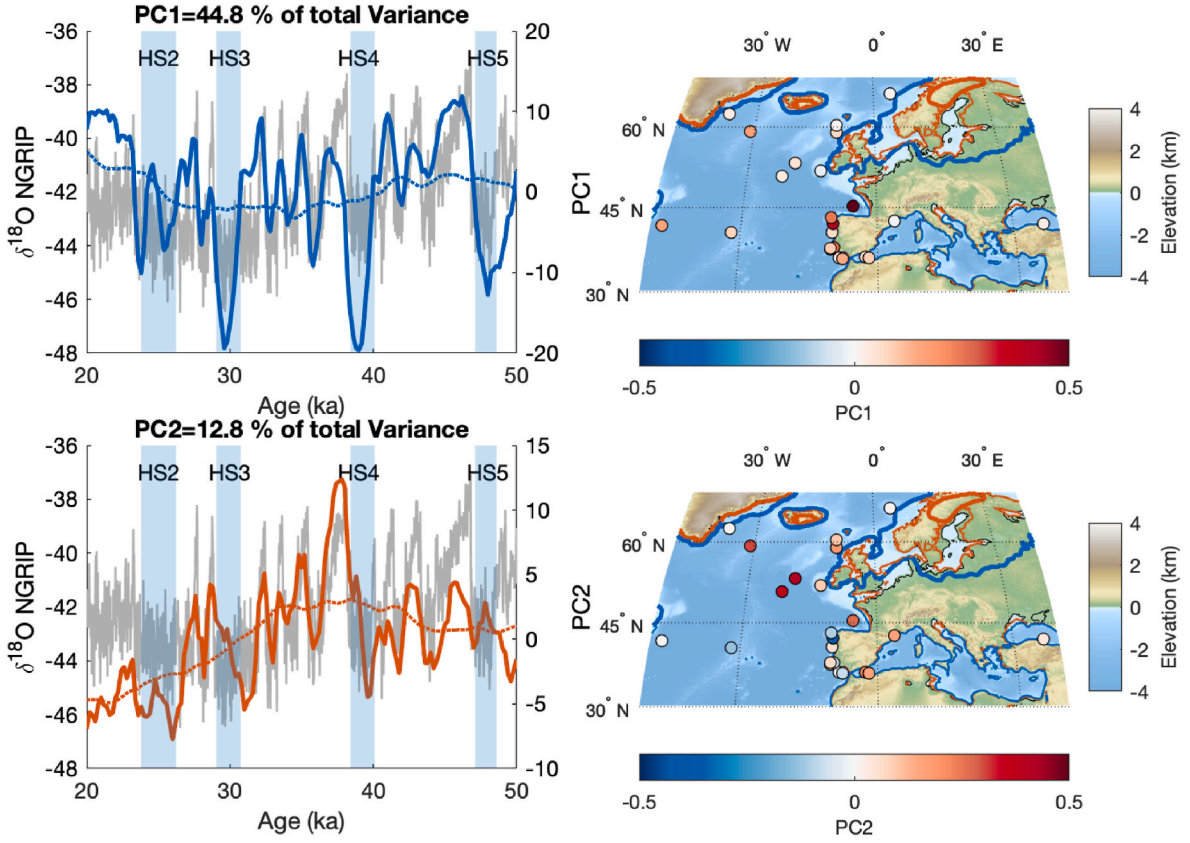

Fig. 2. Principal component analyses of SST records. Time series and loading maps for PC1 (top) and PC2 (bottom) for SST records. The thin dotted line shows the long-term trend based on the 10ka running mean. Blue vertical boxes highlight Heinrich event 2 to Heinrich event 5. Red and blue thick lines on maps show ice sheet extension at 50 and 20 ka respectively (Gowan et al., 2021). Thin red and blue lines represent coastlines at 50 ka and 20 ka respectively (Gowan et al., 2021). The grey background time series represent $\delta^{18}O$ of NGRIP ice core on GICC05 timescale (Wolff et al., 2010).

Table 1
Definition of megabiomes based on characteristic pollen taxa. Details of vegetation types, local names and plant functional types (PFT) of the megabiomes are available in (Fletcher et al., 2010). Additional elements as compared to Fletcher et al. (2010) are underlined.

Warm temperate forest	*Quercus* evergreen type, *Quercus suber* type, *Buxus, Olea, Hedera, Pistacia, Phillyrea, Cistus, Coriaria myrtifolia, Myrtus,* Cannabaceae, *Castanea, Celtis, Fraxinus ornus, Juglans, Ostrya, Platanus, Pterocarya,* Rhamnaceae, *Tamarix, Vitis, Lonicera, Daphne, Ilex, Rhus, Ceratonia, Jasminum, Ligustrum, Syringa, Zelkova, Ziziphus,* Moraceae, *Argania, Quercus cerris, Ceratonia, Arbutus, Erica arborea, Myrtus, Nerium oleander,* Cistaceae, Thymeleaceae, *Laurus, Paliurus, Cercis, Rhododendron, Maytenus, Chamaerops.*
Temperate forest	*Quercus* deciduous type, *Alnus, Acer, Corylus, Fagus, Carpinus, Fraxinus, Ulmus, Tilia, Viscum, Salix, Viburnum, Sambucus, Cornus, Euonymus, Frangula, Myrica, Prunus, Sorbus, Taxus, Cedrus, Liquidambar, Zelkova, Aesculus.*
Boreal forest	*Picea, Abies, Larix, Betula, Populus.*
Eurythermic conifers	*Pinus* (excluded from pollen sum in marine records), *Juniperus*, Cupressaceae.
Grassland and dry shrubland	Ericaceae, *Calluna, Hippophae, Ulex*, Poaceae, Cyperaceae, *Helianthemum*, other non-arboreal pollen
Xerophytic steppe	*Artemisia*, Amaranthaceae, *Ephedra, Lygeum, Noaea.*
Tropical elements	*Podocarpus, Acacia, Acacia albida,* Combretaceae, Zygophyllaceae, Iacinaceae, Salvadoraceae, *Alchornea, Blepharis, Boerhavia, Borreria, Cleome, Diospyros, Grewia, Hagenia, Justicia, Leucaena, Maerua,* Sapindaceae, Sapotaceae.

analyses. To address this, we analyze the normally distributed variability of log(Tf/nTf*100), with Tf and nTf expressed as percentages of total assemblage. This approach is analogous to the arboreal pollen to non-arboreal pollen ratio (AP/NAP) described by Favre et al. (2008).

Some palynological records contain samples with low counts (fewer than 100 grains, e.g. Britzius et al. (2024)), leading to higher uncertainty. To mitigate this, we applied temporal binning to reduce resolution and improve reliability. Biome classification results are provided in the supplementary data.

3. Results

3.1. Chronological constraints

We analyzed the chronological uncertainties associated with each archive and ensured they were consistently propagated through the age-depth models. The average chronological standard error (2σ) is generally below 2 ka in marine archives, whereas it ranges from 2 to 4 ka in continental records (Fig. 1, see also Supplementary Table 1). This disparity limits the resolution at which millennial-scale variability can be reliably identified in continental records, particularly when attempting regional comparisons. As a result, only long-term trends can be robustly inferred from the combined analyses of continental archives at a regional scale. Nevertheless, millennial-scale variability can still be analyzed at the site level, even if the variability is not perfectly aligned with the Greenland ice core chronology. In contrast, many marine archive age models—particularly those from the earlier part of the studied interval, where radiocarbon dating is reaching its limit—were partially tuned to the NGRIP $\delta^{18}O$ record. This tuning facilitates direct comparisons between marine proxy signals and Dansgaard-Oeschger–Heinrich (DO-H) variability.

3.2. Sea surface temperature variability

We analyzed the spatiotemporal structure of the sea surface temperature variability over the 50-20 ka period using a principal component analysis. SST time series were first binned at a 200-year resolution and linearly interpolated onto the same 200-year resolution. Gaps exceeding 1000 years were treated as missing values, and only records covering at least 50 % of the period of interest were retained for analysis (Supplementary Fig. S1). Each selected record was centered with the mean temperature during the studied period, and missing values were replaced with zeros to nullify their weight in the PCA.

The first principal component (PC1) of SST explains 45 % of the total variance, with higher loadings concentrated near the Iberian margin (Fig. 2). PC1 displays millennial-scale variability consistent with DO variability, although Heinrich stadials are more strongly expressed than non-Heinrich stadials (Fig. 2 and Supplementary Fig. S2). The second principal component (PC2), accounting for nearly 13 % of the variance, reflects additional millennial-scale variations that partially align with the NGRIP $\delta^{18}O$ record combined with a long-term cooling trend. This long-term trend in SST records is most pronounced in the northeastern Atlantic, where SSTs declined by up to 6 °C over the 50–20 ka interval (Supplementary Fig. S3). It is worth noting that the SST PC2 appears to show modest increases during some Heinrich stadials.

3.3. Pollen-based vegetation changes

We applied the same analytical pipeline used for the SST records to the log-transformed ratio of temperate forest to non-temperate forest taxa, log(Tf/nTf × 100). In addition to being centered, the log(Tf/nTf × 100) series was also normalized to the variance of the time series before performing the PCA. The first principal component of log(TF/nTF × 100), hereafter named Biome PC1, accounts for 26 % of the total variance and reveals a long-term decline in temperate forest cover between 45 and 20 ka (Fig. 3). Additionally, reductions in temperate forest taxa are particularly notable during Heinrich stadials in Biome PC1. Sites with the highest loadings on Biome PC1 form a broad arc spanning the Iberian margin, the Alboran Sea, the Italian peninsula, the Aegean Sea, and the southeastern Mediterranean basin. Moreover, the slope of the long-term linear trend presents a clear longitudinal gradient, with most negative values observed at the easternmost sites (Supplementary Fig. S3; see also Fig. 7), indicating a more pronounced vegetation shift in these regions. Due to larger chronological uncertainties in terrestrial records—particularly when aggregated—millennial-scale variations in Biome PC1 are less reliably resolved, though individual site-level trends may still hold significance.

The second principal component (Biome PC2), explaining 11.5 % of the variance, captures millennial-scale variability that is most strongly expressed in western marine archives. This component mirrors the structure of Greenland temperature fluctuations and shows reduced temperate forest representation during Heinrich stadials compared to non-Heinrich stadials. In addition to this short-term variability, Biome PC2 exhibits a rising trend from 50 to ~30 ka, followed by a decline toward the Last Glacial Maximum (LGM).

4. Discussion

We begin the discussion by comparing long-term (multi-millennial) trends in the principal components of SST and pollen datasets—defined using a 10 ka running mean (see Supplementary Fig. S2)—to orbital forcings and ice sheet dynamics. We then compare the residual with millennial-scale variability mechanisms, such as oceanic circulation changes or pCO_2 fluctuations. Finally, we consider how the environmental variability described here may have shaped the distribution, adaptation, and cultural development of human populations in Western Europe during the last glacial period focusing on the Châtelperronian and Uluzzian technocomplexes.

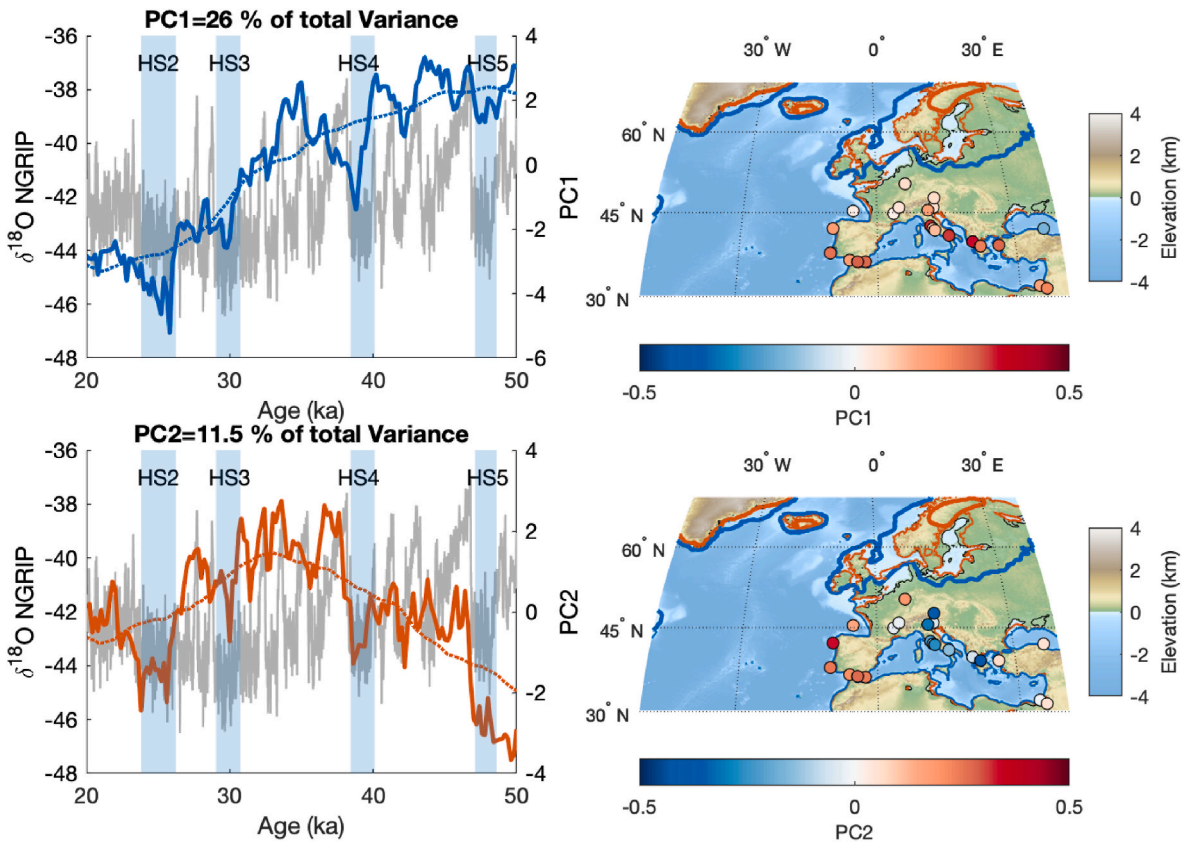

Fig. 3. Principal component analyses of Tf/nTf records. Time series and loading maps for PC1 and PC2 for Tf/nTf records. Blue vertical boxes highlight Heinrich event 2 to Heinrich event 5. Red and blue thick lines on maps show ice sheet extension at 50 and 20 ka respectively (Gowan et al., 2021). Thin red and blue lines represent coastlines at 50 and 20 ka respectively (Gowan et al., 2021). Grey background time series represent $\delta^{18}O$ of NGRIP ice core on GICC05 timescale (Wolff et al., 2010).

4.1. Multi-millennial trends of climate during 50–20 ka BP

4.1.1. Latitudinal climate gradients and the role of seasonal insolation forcing

PC1 of SSTs indicates the absence of a clear and consistent multi-millennial trend along the Iberian margin (between 35 and 45°N), while PC2 of SSTs indicates a long-term decreasing trend that is strongest in the North Atlantic open ocean (50–60°N, Fig. 2, see also Supplementary Fig. S3). This latitudinal pattern coincides with the latitudinal pattern of mean annual insolation that decreased between 50 and 30 ka north of 43°N due to changes in obliquity, remained stable around 43°N, but increased further south (Fig. 4, see also Fig. S4). An enhanced long-term trend at northernmost sites is consistent with a stronger expression of interstadials during obliquity maxima, which coincides with the mean annual insolation maximal value at high latitudes (Fletcher and Sánchez Goñi, 2008; Sánchez Goñi et al., 2008; Fletcher et al., 2010). However, the rise of mean annual insolation at high latitudes between 30 and 20 ka is not associated with temperature change (PC2 of SSTs, Fig. 4), suggesting the influence of other mechanisms at that time.

As the ocean is stratified in summer, a drop in summer insolation may have been more efficient in cooling mean annual SST than winter insolation. Consequently, mean annual oceanic surface temperatures could be biased toward summer insolation forcings (Laepple and Lohmann, 2009). However, spring insolation may also be an important driver of sea ice melt (Stott et al., 2007), which may influence summer conditions (Kapsch et al., 2014) and impact the mean annual SST of the glacial North Atlantic Ocean. Summer insolation at 60°N reaches a minimum at the LGM consistent with SST PC2 (Fig. 4 and Fig. S4) and correlates with SST PC2 variations at orbital timescales (R = 0.58, Table S3), although the temporal patterns differ with a plateau between 40 and 30 ka. Still, May insolation at 60°N better correlates with SST PC2 (R = 0.96), suggesting that late spring insolation could play a significant role in the northern Atlantic, possibly by affecting sea ice during the melting season. Additionally, there is no clear indication, neither in SST PC1 nor in SST PC2, that precession affects sea surface temperature south of 40°N.

Even if Biome PC1 presents a temporal variability compatible with enhanced interstadial expression during peak obliquity (Fletcher and Sánchez Goñi, 2008; Sánchez Goñi et al., 2008; Fletcher et al., 2010), the spatial pattern (lower loadings and lower slope at northernmost sites) is in contradiction with higher obliquity influence at high latitudes. However, the limited continental records north of 50°N prevent any definitive conclusion on the subject. Moreover, the latitudinal gradient on land cannot be explained by divergent mean annual insolation trends (Fig. S4). The long-term trend is stronger in the southern part of the domain, where mean annual insolation remained constant or increased throughout the studied period. Thus, any impact of decreasing mean annual insolation at higher latitudes must have been indirect. Pollen production by trees commonly happens during spring, which could have biased the pollen records toward spring climate and insolation. The long-term trend in Biome PC2 partly matches with May insolation at 40°N (R = 0.65). A slope change of PC1 also coincides with a drop in May insolation, which may indicate that the growing season insolation plays an important role in regional vegetation reconstructions for that period. Because May insolation directly relates to precession (Fig. 4), high loadings for Biome PC2 in the southwestern part of the domain are consistent with the previously noted influence of precession south of 40°N (Fletcher and Sánchez Goñi, 2008; Fletcher et al., 2010) but contrast with SST proxies variability. The negative Biome PC2 values in

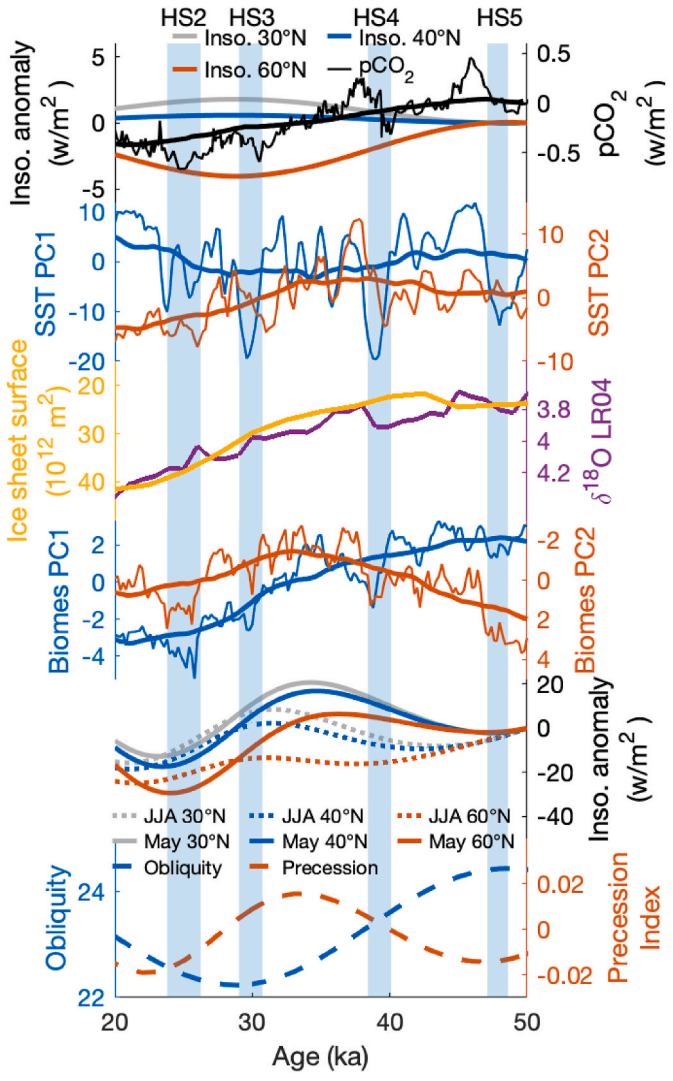

Fig. 4. Mean annual insolation anomaly as compared to 50ka configuration at 30°N, 40°N and 60°N (Berger, 1978; Berger and Loutre, 1991; Huybers and Eisenman, 2006), pCO2 forcing anomaly as compared to 50ka (thick black line shows the 10ka window running mean (Bereiter et al., 2015);); sea surface temperature PC1 and PC2 (thick lines show the 10ka window running mean of the PC1 and PC2). Eurasian ice sheet surface (Gowan et al., 2021) and LR04 benthic $\delta^{18}O$ stack (Lisiecki and Raymo, 2005); Tf/nTf PC1 and PC2. Mean insolation anomaly for summer (JJA) and May at 30°N, 40°N and 60°N; and obliquity and precession index.

Italy and Greece suggest that a longitudinal contrast also impacts precession influence that weakens southeast of the Alps.

4.1.2. Ice sheet surface and atmospheric feedbacks

Although the mean annual insolation spatiotemporal pattern could explain the latitudinal contrasts in long-term SST trends between 50 and 30 ka, SST PC2 diverges from local annual insolation signal at 60°N during the LGM (Fig. 4). The dominant climatic impact of insolation changes on climate is indirect, with summer insolation at high latitudes controlling ice sheet growth that, in turn, strongly impacts global and regional radiative budget. Therefore, the ice sheet influence could have overprinted local insolation changes across our study area, with a combined effect of its impact on the radiative budget (albedo changes), its location, and the preferential longitudinal atmospheric transport through the Westerlies. However, varying orography and albedo may also have impacted atmospheric and oceanic circulation. The long-term decreasing trend of SST PC2 until the LGM better conforms with global climate evolution, thus with the surface of the European ice sheet (R = −0.94, Fig. 4, Table S3) and pCO_2 (R = 0.71), than with mean annual insolation forcing. This interpretation is further supported by the higher SST PC2 loadings near the ice sheet, suggesting a regional impact of the ice sheet surface on SSTs.

On land, Biome PC1 temporal pattern strongly correlates with ice sheet surface variation and pCO_2 (R = −0.96 and 0.97 respectively). While the long-term decrease is more marked close to the ice sheet in the ocean, Biome PC1 presents higher loadings in southern terrestrial sites (Fig. 3), notably southeast of the Alps, away from the ice sheet and the Atlantic Ocean, where the slope of Tf/nTf is also strongly negative. The pattern shown here supports a southward extension of cold and arid climate south of the Alps around 35 ka concurrent with ice sheet growth, probably as a result of interactions of the ice sheet with the alpine arc (Luetscher et al., 2015; Monegato et al., 2017; Pini et al., 2022). The geographical pattern shown here also resembles the signature of changes in the Jet Stream position (Kutzbach et al., 1998) that promotes a climate dipole between northwestern and southeastern Europe (Xu et al., 2024). However, the slope of the trend tends to be lower close to the Atlantic Ocean (Supplementary Figure S3 and Fig. 7), suggesting an oceanic influence inland on multi-millennial timescale as discussed in the following section.

4.1.3. Ocean-continental coupling and the role of the Alps

The long-term trend evidenced at 50–60°N in the ocean and in the southernmost part of the continent fits with the global climatic trend during last glacial with progressively colder conditions and increased ice sheet volume over the course of MIS3 and MIS2 (Fig. 4). Thus, a relatively stable condition during the studied period at mid-latitude is at odds with northern North Atlantic and global climatic evolution. We propose that the local/regional impact of stable mean annual insolation may be the key factor behind these stable SST trends around 40°N. Although, it cannot explain the longitudinal gradient in the expression of the long-term trend on land, which is weaker in westernmost sites, whereas insolation forcing is longitudinally homogenous.

Modern European climate over the continent is considered as oceanic, such as ocean thermal state directly impacts overland conditions. The low amplitude long-term trend in the westernmost sites of Europe close to the Atlantic Ocean (Figs. 3 and 7, see also Fig. S3) agrees with relatively stable SSTs at the same latitudes on multi-millennial timescales (with the exception of the Alboran Sea). This suggests that Western Europe was strongly influenced by the oceanic temperature at mid-latitude through the Westerlies, thus outlining the moderating influence of the mid-latitude Atlantic Ocean over the westernmost European continent during the studied period at multi-millennial timescales. The contrasted long-term trends east and west of the Alps are also consistent with Atlantic influence on European climate. This Atlantic influence contracted westward over time. The development of the Siberian High contributed to the expansion of continental climate in eastern Europe (Obreht et al., 2017a). This likely explains expl the steeper environmental trend over Italian and Greek peninsulas. If true, this also highlights the contrasted sensitivities of oceanic and terrestrial surfaces regarding insolation forcing, ice sheet growth, orography and global climatic variations.

4.2. Millennial-scale trends of climate during 50–20 ka BP

4.2.1. AMOC variability and ocean cooling during stadials

The PC1 of SST records (~45 % of the SST variance) drops significantly during all four Heinrich stadials, while lower amplitude swings are associated with D-O variability. Because Heinrich stadials are associated to a reduction of the AMOC, we compare SST PC1 with the $^{231}Pa/^{230}Th$ ratio at the Bermuda Rise in the Atlantic Ocean, which reflects AMOC intensity (Lippold et al., 2009; Bohm et al., 2015; Henry et al., 2016). Both records display relatively stable values over the studied period, interrupted by millennial-scale drops concomitant with

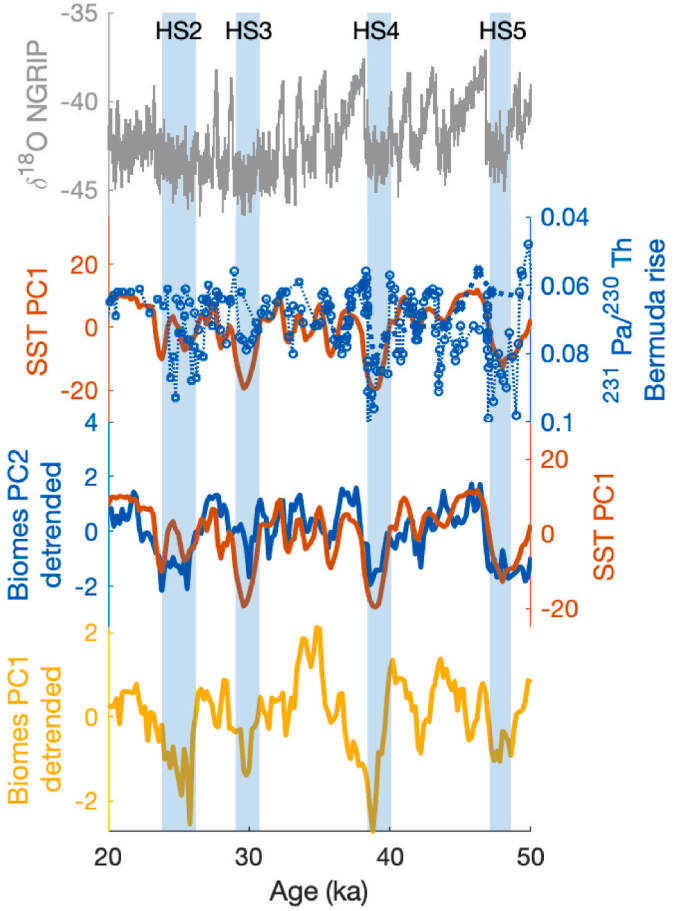

Fig. 5. $\delta^{18}O$ of NGRIP ice core (GICC05 timescale (Wolff et al., 2010)). Sea surface temperature PC1, $^{231}Pa/^{230Th}$ at Bermuda Rise (Lippold et al., 2009; Bohm et al., 2015; Henry et al., 2016). Higher $^{231}Pa/^{230Th}$ indicates less active overturning circulation. Biome PC2 detrended and SST PC1, and Biome PC1 detrended.

stadials, although with higher amplitude during the Heinrich stadials (Fig. 5). This suggests that SST at the Iberian margin was primarily driven by changes in AMOC strength. This is confirmed by modelling studies that consistently indicate reduced temperature in the Northern Hemisphere during weakened AMOC due to reduced northward heat transport (Ganopolski and Rahmstorf, 2001; Liu et al., 2009; Kageyama et al., 2013; Menviel et al., 2014). Moreover, the high variance of temperature proxy records around 45°N (Supplementary Fig. S2) is consistent with latitudinal oscillation of polar front and summer sea ice extent in the north western Atlantic, in pace with AMOC variations (Pedro et al., 2022). An enhanced signature of Heinrich stadials at the Iberian margin is also consistent with a southward displacement of the polar front compared to non-Heinrich stadials (Bard et al., 1987; Eynaud et al., 2009; Pedro et al., 2022; Davtian and Bard, 2023).

4.2.2. Ocean–land coupling and vegetation shifts

The analyses of the Tf/nTf ratio can be used to constrain the extent of oceanic influence on continental vegetation. When the long-term trend is removed from Biome PC2, the correlation between the detrended Biome PC2 and SST PC1 reaches 0.68 (Fig. 5). Both records show millennial-scale variability in phase with DO variability and strong Heinrich stadials. Since the millennial-scale signal in Biome PC2 mainly results from the variability of marine sediment core records (see section 3.3), we cannot exclude that varying transport (e.g. aerial versus water transport) and sedimentary processes over the Iberian margin partially imposed a temporal pattern on marine-based pollen records independently from environmental factors affecting pollen production and preservation. Changes in oceanic circulation and latitudinal oscillation of the frontal zone may explain the pollen deposition pattern, although this process is not considered to be dominant (Koreneva, 1966; Stanley, 1966; Sánchez Goñi et al., 1999; Naughton et al., 2007; Sanchez Goñi et al., 2018). Consequently, Biome PC2 more likely reflect changes in climatic conditions.

Oceanic influence in western Europe during the last glacial period has been identified even in areas far from the Atlantic Ocean, such as the Black Sea (Wegwerth et al., 2015). However, its impact on the continent remains uncertain. The high Biome PC2 loadings around the Iberian Peninsula, which are consistent with the latitudinal distribution of SST PC1 loadings, confirm that continental vegetation was indeed affected by oceanic climate in western Europe. Unfortunately, the geographical extension of this influence is difficult to ascertain due to numerous factors. First, the presence of the ice sheet over northern Europe strongly affected sedimentation processes over most of the continent, so that long, high-resolution glacial records are rare. This absence of suitable records in the northern sector of our study area prevents a rigorous comparison of the latitudinal structure of marine and terrestrial records millennial-scale variability. Chronological uncertainties are also larger for terrestrial records (Fig. 1). Nevertheless, millennial-scale variability similar to DO variability has been recorded in numerous terrestrial sites of western Europe (e.g. de Beaulieu and Reille, 1984; Guiot et al., 1993; Leroy et al., 1996; Allen et al., 1999; Brunck et al., 2016; Sirocko et al., 2016; Moseley et al., 2020; Kappenberg et al., 2021; Pini et al., 2022; Badino et al., 2023; Britzius et al., 2024) even if their chronologies often prevent aligning the observed climate swings to specific stadial or interstadial. The millennial-scale variations of Biome PC1 show slightly reduced values during Heinrich stadials, which could indicate widespread impact on the continent although with low confidence. However, the temporal pattern evidenced in the ocean, with more strongly expressed Heinrich stadials relative to non-Heinrich stadials (SST PC1) cannot be systematically identified visually in individual terrestrial archives biome distribution variations (Supplementary Fig. S5), even if accounting for chronological uncertainties, suggesting that this mode of variability does not prevail in the eastern sector of the studied domain, away from the Atlantic Ocean.

Additionally, the increasingly challenging conditions for temperate trees within glacial refugia (mainly in the three Mediterranean Peninsula, i.e. Iberia, Italy, Balkans) and the recurrent stadials likely had a cumulative negative effect on the ability of trees to recolonize Europe, progressively reducing their distribution. Soil regeneration may have been similarly impacted, as successive glacial conditions would have required increasingly longer periods for soil formation and stabilization, further limiting forest resilience and recovery and contributing to temperate forest decreasing trend as seen in Biome PC1. However, this process may have been less important in the Iberian Peninsula due to the dampening effect of the Atlantic Ocean (Fig. 7), explaining the longitudinal trend in forest cover reduction.

4.2.3. Antarctic influence and bipolar seesaw dynamics

The thermal bipolar seesaw mechanism leads to asymmetric temperature trends between hemispheres, in relation to changes in AMOC strength. When the AMOC abruptly slows down, northward heat transport is reduced, leading to the progressive buildup of heat in the Southern Hemisphere and cooling in the Northern Hemisphere. When the AMOC resumes, the excess heat in the south is progressively released northward, which imposes a characteristic triangular pattern on the Southern Hemisphere thermal states with increasing temperature during Heinrich stadials. Although mechanisms are complex (Zheng et al., 2021), millennial-scale atmospheric pCO_2 variations clearly follow the Southern Hemisphere temperature temporal pattern.

The timing of the PC2 of SSTs millennial-scale variability contrasts with that of SST PC1 (Figs. 2 and 6). In particular, it indicates warming temperature trends over the course of Heinrich stadials at 40 and 30 ka

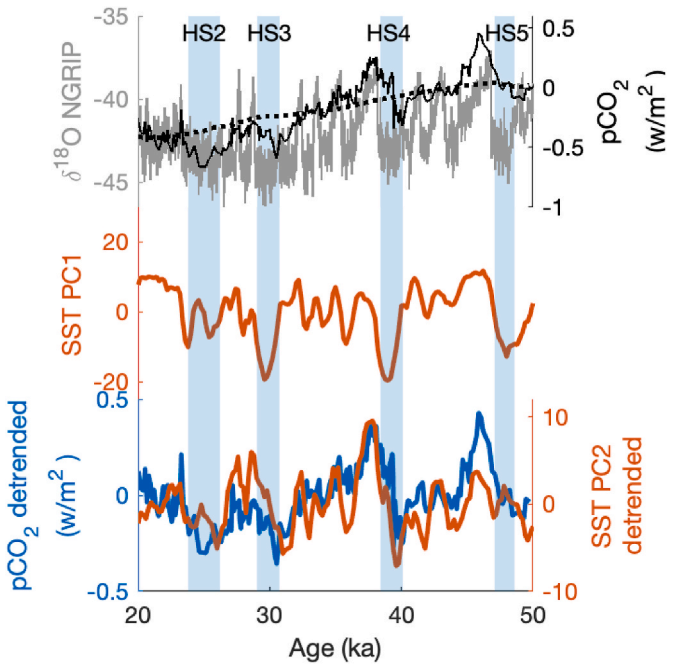

Fig. 6. pCO2 forcing anomaly as compared to 50ka (AICC2012 age scale (Veres et al., 2013), compatible with GICC05; thick black dotted line shows the 10ka window running mean (Bereiter et al., 2015);) and $\delta^{18}O$ of NGRIP ice core (GICC05 timescale (Wolff et al., 2010)). Sea surface temperature PC1, detrended sea surface temperature PC2, and detrended pCO2 forcing anomaly.

BP and correlates with pCO_2 variations in the atmosphere, and Antarctic temperature (see also Rasmussen et al., 2016), while PC1 of SSTs is synchronized with North Atlantic cold stadials (Fig. 6). Thus, Antarctic-like variability, as theorized through the bipolar seesaw, may not only affect the Southern Hemisphere but might reach the mid-to high latitudes of the North Atlantic open ocean. The Antarctic signal in the northern Atlantic may result from a subdued expression of the southern branch of the bipolar seesaw through the northward transport of surface water originating in the southern hemisphere or from exchanges with intermediate water (Rasmussen et al., 2016). The southern hemisphere timing evidenced in the northern Atlantic could also result from the direct impact of pCO_2 on the global radiative budget that is correctly deconvoluted with the principal component analyses, in a region strongly affected by DO-H variability. Significant changes in global sea level during MIS3 (25–30 m) also followed a timing similar to Antarctic-like millennial scale variability (Shackleton et al., 2000; Rohling et al., 2008, 2009), with a contribution of both hemisphere ice sheets (Hill et al., 2006; Rohling et al., 2008). Therefore, the MIS3 northern hemisphere ice sheet extension may have imposed Antarctic timing on SST PC2 in the northern Atlantic.

4.3. *Palaeoenvironmental constraints on human evolution*

4.3.1. *Long-term environmental trends and cultural divergence*

The Middle to Upper Palaeolithic transition (45–35 ka BP), marked by the gradual replacement or assimilation of Neanderthals by anatomically modern humans, is a pivotal phase in European prehistory (Bar-Yosef, 2002; Higham et al., 2014; Hublin, 2015; Zilhão et al., 2024). This period has spurred significant research into the interactions between cultural change and environmental conditions (d'Errico and Sánchez Goñi, 2003; Müller et al., 2011; Höbig et al., 2012; Stewart and Stringer, 2012; Banks et al., 2013; Obreht et al., 2017b; Ludwig et al., 2018; Columbu et al., 2020; Sánchez Goñi, 2020; Shao et al., 2021, 2024; Fourcade et al., 2022a, b; Klein et al., 2023; Higham et al., 2024; Rathmann et al., 2024; Timmermann et al., 2024; Zilhão et al., 2024).

Western Europe, particularly regions near the Atlantic Ocean, experienced relatively stable climatic conditions at multi-millennial scales. This contrasts with southeastern Europe—notably Italy and Greece—which underwent more pronounced environmental shifts, as indicated by strong long-term vegetation trends (Fig. 7). Interestingly, these differences align with archaeological patterns: while Mousterian industries were widespread during the middle Palaeolithic, the Uluzzian culture emerged later in Italy and Greece, distinctively from the Châtelperronian industry in the Atlantic region (Marciani et al., 2025). In later phases of the Upper Palaeolithic, the Epigravettian industries in Italy and Balkans also diverged from the Solutrean and Magdalenian ones in Western Europe (Djindjian et al., 1999; Hussain and Floss, 2014; Banks et al., 2024).

The pronounced long-term climatic gradient southeast of the Alps likely contributed to cultural isolation. This reinforced distinct technological trajectories, even when chronologies overlapped (Marciani et al., 2025). The Alps, acting as a biogeographic and climatic barrier, may have constrained migration and cultural exchanges in the narrow corridor south of the mountain arc (Tomasso and Porraz, 2016; Obreht et al., 2017b). Thus, Western Europe may have homed a more favorable multi-millennial climate trend for human population closer to the ocean, possibly explaining contrasted long-term trend in cultural evolution (Fig. 7).

4.3.2. *Heinrich stadials and human mobility/adaptation*

During Heinrich stadials, the decrease in temperate forest taxa along the western European coast was more pronounced than during D-O stadials, as indicated by Biome PC2. This pattern reflects the latitudinal oscillation of the oceanic front driven by AMOC disruption during last glacial period. Although Biome PC1 also shows a reduction in temperate forest pollen proportion during Heinrich stadials, this signal is inconsistent outside coastal Atlantic regions, underscoring the regional variability of these events. As a result, the timing and amplitude of environmental stressors impacting human population varied across western Eurasia, with the strongest effects felt near the Atlantic margin due to AMOC changes (Fig. 7).

The influence of Heinrich stadials on human populations remains debated. Some studies suggest that the expansion of steppe environments during these cold phases, espescially Heinrich events, supported large herbivore populations. In turn, this may have favored hunter gatherer subsistence strategies (d'Errico et al., 2006; Sánchez Goñi, 2020). Others suggest a stagnation in population growth during these periods, as seen with the Aurignacian during Heinrich stadial 4, with increased mobility occurring during the transitions from stadial to interstadial periods (Shao et al., 2024). Similarly the deglaciation period in the Early Pleistocene has been suggested as the best time for hominins to migrate into western Europe following herbivore herds (Leroy et al., 2011). Further support for demographic shifts comes from phenotypic data pointing at enhanced population turnover around 28 ka, coinciding with the end of Heinrich 3 (Rathmann et al., 2024). Thus, palaeontological records are consistent with enhanced climatic impact of Heinrich stadials as compared to stadials over Western Europe as seen in proxy records, although the modality remains debated.

4.3.3. *Archaeological evidence and regional heterogeneity*

The high density of artefacts, the cultural innovations, and the recorded events in westernmost Europe may partly reflect the moderating influence of the Atlantic Ocean, which could have supported more stable subsistence strategies for hominin populations. However, potential sampling biases must also be acknowledged. Recent research shows that modern land cover, building and mining activities, better predict the distribution of archaeological sites in Western Europe than factors relevant to Palaeolithic settlement patterns (Boemke et al., 2023). Additionally, significant portions of the landscapes once inhabited by Pleistocene hunter-gatherers, such as the North Sea basin and various coastal regions, are now submerged, resulting in substantial

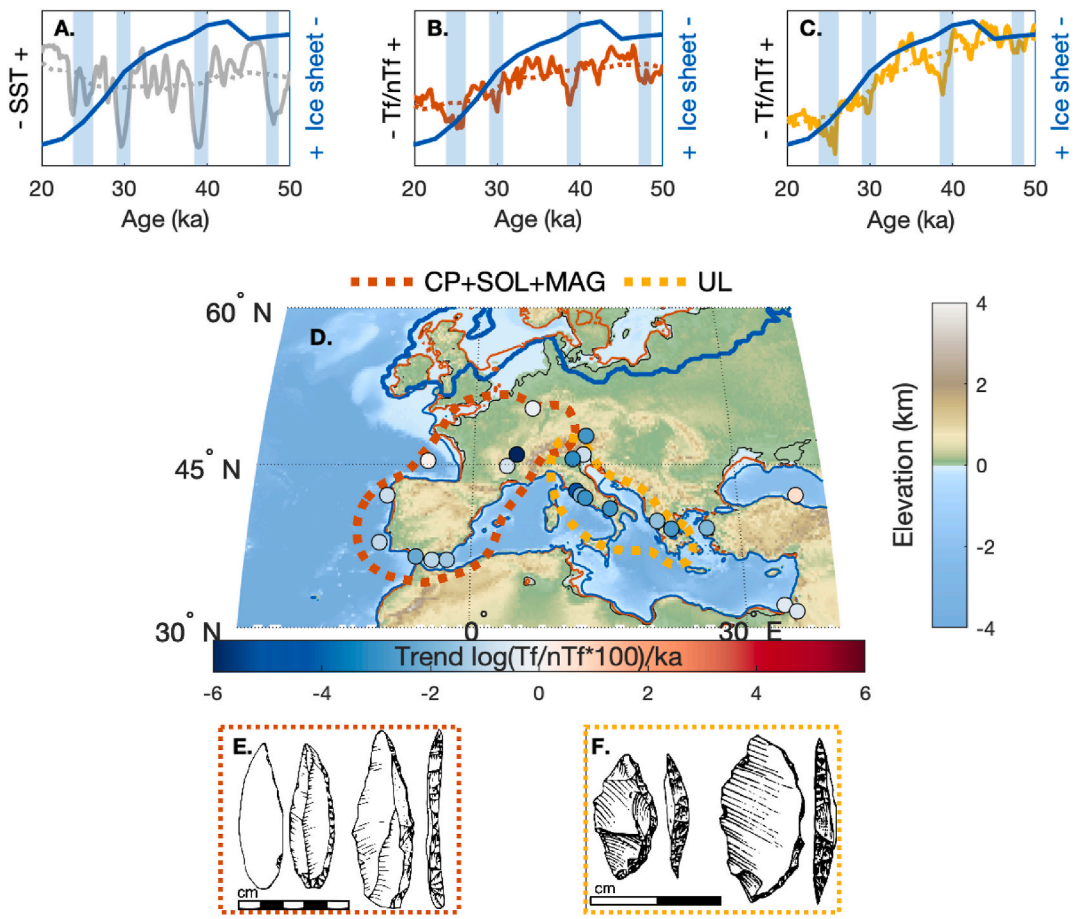

Fig. 7. Schematic representation of climatic trends in western Europe. A, B and C: Ice sheet surface (blue curve). A. SST at mid latitudes displaying stable long-term trend over the studied period, and high amplitude Heinrich stadial (SST PC1); B. Tf/nTf in westernmost pollen records with small amplitude multi-millennial trend and high amplitude Heinrich stadials (Biome PC1 in addition to millennial-scale variability of Biome PC2); C. Tf/nTf with high amplitude multi-millennial trend and low amplitude Heinrich stadials over Italian and Greek peninsulas (Biome PC1). D. Linear trend slope in Tf/nTf highlighting reduced decreasing trend in westernmost sites as compared to Italy and Greece. Extension area for Châtelperronian (CP), Solutrean (SOL), and Magdalenian (MAG, red), and Uluzzian (UL, yellow) (ROCEEH Out of Africa Database, Kandel et al., 2023). E. Châtelperron points, Grotte du Renne, France after (Movius Jr, 1969; Klein, 2000), characteristic of the Châtelperronian industry. F. Lunates, Uluzzo C Rock Shelter, south-eastern Italy after (Borzatti von Löwenstern, 1965; Silvestrini et al., 2021), characteristic of Uluzzian complex.

geographical biases in the distribution of the Palaeolithic archaeological record (Roebroeks, 2014).

Despite these limitations, our analyses of continental proxies suggest that inland regions may have experienced different climatic pressures than Atlantic coastal zones. Notably, the influence of Heinrich stadials appears to have been weaker away from the Atlantic Ocean, whereas long-term environmental trends likely played a stronger influence in southern Europe (notably Italy and Greece), as reflected in SST PC1 and Biome PC1 (Figs. 2, 3 and 7). These regional differences in climatic dynamics may have played a crucial role in shaping hominin resilience, mobility, and innovation during the Middle and Upper Palaeolithic as well as during the final Palaeolithic (Schmidt et al., 2024).

Given this spatial heterogeneity, future research into prehistoric population dynamics should incorporate regionally specific climate reconstructions and explicitly account for regional environmental conditions. Aligning archaeological patterns with locally resolved palaeoenvironmental data provides a more robust framework for understanding human adaptations to glacial climate variability than reliance on Greenland ice core data alone.

5. Conclusions

This study provides new insights into sea surface temperature and terrestrial vegetation variability across Europe and the Mediterranean Basin during the last glacial period, focusing on the critical 50–20 ka BP interval—a phase marked by profound climatic shifts and significant human evolutionary transitions.

At multi-millennial timescale, sea surface temperature declined markedly in the northernmost part of the northern Atlantic near the ice sheet, while mid-latitude SSTs (~40–45°N) remained comparatively stable. This stability, driven by relatively constant mean annual insolation, likely buffered climatic extremes in parts of Western Europe, especially those closest to the ocean, where the Last Glacial Maximum was not drastically colder than MIS3. In contrast, regions southeast of the Alps experienced pronounced cooling and drying until LGM, influenced by ice sheet expansion, shifting atmospheric circulation, and topographic barriers. These patterns reveal the differentiated sensitivity of terrestrial and marine realms to orbital forcing and ice sheet dynamics, and suggest that geographic and climatic barriers—such as the Alps—may have contributed to cultural isolation and divergence. This indeed coincides with the archaeological record, which shows distinct regional developments, including the emergence of the Uluzzian in southern Europe and the Châtelperronian in the west.

At millennial timescale, SST records show high-amplitude oscillations in pace with Dansgaard-Oeschger variability, with particularly strong cooling during Heinrich stadials along the Iberian margin. These cold episodes were linked to disruptions of the Atlantic Meridional Overturning Circulation (AMOC), which triggered sharp temperature

drops and reduced forest cover in adjacent coastal regions. The data demonstrate that AMOC weakening had a major influence on regional environments and likely shaped human ecosystems along the western European margin. However, our analysis showed that these effects were less pronounced inland, where long-term environmental pressures, rather than abrupt events, appear to have played a more dominant role. This spatial heterogeneity implies that prehistoric populations across Europe experienced vastly different environmental pressures depending on their geographic context.

Importantly, this study emphasizes the dual role of the Atlantic Ocean during the last glacial period. It is both a stabilizing force at orbital scales and a driver of pronounced variability at millennial scales. These results highlight the value of integrating high-resolution marine and terrestrial proxies. This approach allows for a better understanding of how environmental dynamics influenced human prehistory. Rather than viewing climate as a uniform forcing agent, our results support a more nuanced perspective in which regional and temporal variability modulated opportunities and constraints for population resilience, mobility, and cultural innovation. Coastal regions buffered by oceanic influence may have offered more stable conditions for hominin subsistence, potentially contributing to higher archaeological innovation (and visibility) in westernmost Europe.

Future work should further investigate the complex interplay between climatic variability and human behavior through regionally resolved, high-resolution, and interdisciplinary datasets. By coupling palaeoclimatic reconstructions with archaeological evidence and demographic modeling, we can more accurately trace the pathways through which climate shaped human trajectories during the Late Pleistocene—and refine our understanding of the ecological constraints and adaptive strategies of Palaeolithic populations.

Author contributions

O.C., T.D. and E.B. conceptualized the study and participated in funding acquisition. curated data; performed analyses, wrote the original draft and produced figures; , S.L., M.C., D.F. all participated in writing, reviewing and editing.

Declaration of competing interest

The authors declare that they have no known competing financial interests or personal relationships that could have appeared to influence the work reported in this paper.

Acknowledgements

OC was supported by ANR NEHOS (PI: T. Devièse, ANR-22-CE27-0016) and ANR MARCARA (PI: E. Bard, ANR-21-CE01-0023). The data collection benefited from a database developed within CYCLOCARB MSCA (PI: O. Cartapanis, MSCA No 897046). MC was supported by the German Federal Ministry of Education and Research (BMBF) as a Research for Sustainability initiative (FONA; https://www.fona.de/en) through the PalMod Phase III project (grant no. 01LP2308B). We are grateful to S. Badino, J. S. Carrión, P. Stojakowits, C. Mayr, and S. Britzius who directly contributed their data. We thank Editor I. Hendy and one anonymous reviewer for their constructive feedback and insightful comments, which greatly improved the clarity and quality of this manuscript.

Appendix A. Supplementary data

Supplementary data to this article can be found online at https://doi.org/10.1016/j.quascirev.2025.109429.

Data availability

All data and/or code is contained within the submission.

References

Allen, J.R.M., Brandt, U., Brauer, A., Hubberten, H.-W., Huntley, B., Keller, J., Kraml, M., et al., 1999. Rapid environmental changes in southern Europe during the last glacial period. Nature 400, 740–743.

Andersen, K.K., Svensson, A., Johnsen, S.J., Rasmussen, S.O., Bigler, M., Röthlisberger, R., Ruth, U., et al., 2006. The Greenland Ice Core Chronology 2005, 15–42ka. Part 1: constructing the time scale. Critical Quaternary Stratigraphy 25, 3246–3257.

Badino, F., Pini, R., Ravazzi, C., Chytrý, M., Bertuletti, P., Bortolini, E., Dudová, L., et al., 2023. High-resolution ecosystem changes pacing the millennial climate variability at the Middle to Upper Palaeolithic transition in NE-Italy. Sci. Rep. 13, 12478.

Banks, W.E., d'Errico, F., Zilhão, J., 2013. Human–climate interaction during the early upper paleolithic: testing the hypothesis of an adaptive shift between the proto-aurignacian and the early aurignacian. J. Hum. Evol. 64, 39–55.

Banks, W.E., Vignoles, A., Lacarrière, J., Morala, A., Klaric, L., 2024. A hierarchical bayesian examination of the chronological relationship between the noaillian and rayssian phases of the French middle gravettian. Quaternary 7.

Bard, E., Arnold, M., Maurice, P., Duprat, J., Moyes, J., Duplessy, J.-C., 1987. Retreat velocity of the North Atlantic polar front during the last deglaciation determined by 14C accelerator mass spectrometry. Nature 328, 791–794.

Bard, E., Rostek, F., Jean Louis, T., Gendreau, S., 2000. Hydrological impact of Heinrich events in the subtropical northeast atlantic. Science (New York, N.Y.) 289, 1321–1324.

Bar-Yosef, O., 2002. The upper paleolithic revolution. Annu. Rev. Anthropol. 31, 363–393.

de Beaulieu, J.-L., Reille, M., 1984. The pollen sequence of les échets (France): a new element for the chronology of the upper Pleistocene. Géogr. Phys. Quaternaire 38, 3–9.

Bereiter, B., Eggleston, S., Schmitt, J., Nehrbass-Ahles, C., Stocker, T.F., Fischer, H., Kipfstuhl, S., Chappellaz, J., 2015. Revision of the EPICA Dome C CO2 record from 800 to 600 kyr before present. Geophys. Res. Lett. 42, 542–549.

Berger, A.L., 1978. LONG-TERM variations of caloric insolation resulting from earths orbital elements. Quat. Res. 9, 139–167.

Berger, A.L., 1981. The astronomical theory of paleoclimates. In: Berger, A. (Ed.), Climatic Variations and Variability: Facts and Theories: NATO Advanced Study Institute First Course of the International School of Climatology, Ettore Majorana Center for Scientific Culture. Springer Netherlands, Dordrecht, Erice, Italy, pp. 501–525. March 9–21, 1980.

Berger, A., Loutre, M.F., 1991. Insolation values for the climate of the last 10 million years. Quat. Sci. Rev. 10, 297–317.

Boemke, B., Maier, A., Schmidt, I., Römer, W., Lehmkuhl, F., 2023. Testing the representativity of Palaeolithic site distribution: the role of sampling bias in the european upper and Final Palaeolithic record. Quat. Sci. Rev. 316, 108220.

Bohm, E., Lippold, J., Gutjahr, M., Frank, M., Blaser, P., Antz, B., Fohlmeister, J., et al., 2015. Strong and deep Atlantic meridional overturning circulation during the last glacial cycle. Nature 517, 73–76.

Bond, G., Heinrich, H., Broecker, W., Labeyrie, L., McManus, J., Andrews, J., Huon, S., et al., 1992. Evidence for massive discharges of icebergs into the North Atlantic ocean during the last glacial period. Nature 360, 245–249.

Borzatti von Löwenstern, E., 1965. La grotta-riparo di Uluzzo C. Rivista di scienze preistoriche 1–31.

ter Braak, C.J., van Dame, H., 1989. Inferring pH from diatoms: a comparison of old and new calibration methods. Hydrobiologia (The Hague) 178, 209–223.

Britzius, S., Dreher, F., Maisel, P., Sirocko, F., 2024. Vegetation patterns during the last 132,000 Years: a synthesis from twelve eifel maar sediment cores (Germany): the ELSA-23-pollen-stack. Quaternary 7.

Brunck, H., Sirocko, F., Albert, J., 2016. The ELSA-Flood-Stack: a reconstruction from the laminated sediments of Eifel maar structures during the last 60000years. Global Planet. Change 142, 136–146.

Cartapanis, O., Jonkers, L., Moffa-Sanchez, P., Jaccard, S.L., de Vernal, A., 2022. Complex spatio-temporal structure of the Holocene thermal maximum. Nat. Commun. 13, 5662.

Charton, L., Combourieu-Nebout, N., Bertini, A., Lebreton, V., Peyron, O., Robles, M., Sassoon, D., Moncel, M.-H., 2025. Vegetation and climate changes during the Middle to Upper Palaeolithic transition in the southwestern Mediterranean: what happened to the last Neanderthals during Heinrich stadial 4? Quat. Sci. Rev. 359, 109345.

Columbu, A., Chiarini, V., Spötl, C., Benazzi, S., Hellstrom, J., Cheng, H., De Waele, J., 2020. Speleothem record attests to stable environmental conditions during Neanderthal–modern human turnover in southern Italy. Nature Ecology & Evolution 4, 1188–1195.

Conte, M.H., Sicre, M.-A., Rã¼hlemann, C., Weber, J.C., Schulte, S., Schulz-Bull, D., Blanz, T., 2006. Global temperature calibration of the alkenone unsaturation index (UKâ€²37) in surface waters and comparison with surface sediments. Geochem. Geophys. Geosystems 7.

Davtian, N., Bard, E., 2023. A new view on abrupt climate changes and the bipolar seesaw based on paleotemperatures from Iberian Margin sediments. In: Proceedings of the National Academy of Sciences, vol.120, e2209558120.

Djindjian, F., Kozlowski, J., Otte, M., 1999. Le paléolithique supérieur en Europe. A. Colin.

Dommenget, D., 2009. The Ocean's role in continental climate variability and change. J. Clim. 22, 4939–4952.
d'Errico, F., Sánchez Goñi, M.F., 2003. Neandertal extinction and the millennial scale climatic variability of OIS 3. Quat. Sci. Rev. 22, 769–788.
d'Errico, F., Sanchez Goñi, M., Vanharen, M., 2006. L'impact de la variabilité climatique rapide des OIS3-2 sur le peuplement de l'Europe [CrossRef Partial][Check multiple vol, first-page, last-page, msc3].
Eynaud, F., de Abreu, L., Voelker, A., Schönfeld, J., Salgueiro, E., Turon, J.-L., Penaud, A., et al., 2009. Position of the Polar Front along the western Iberian margin during key cold episodes of the last 45 ka. Geochem. Geophys. Geosystems 10 n/a-n/a.
Favre, E., Escarguel, G., Suc, J.-P., Vidal, G., Thévenod, L., 2008. A contribution to deciphering the meaning of AP/NAP with respect to vegetation cover. Rev. Palaeobot. Palynol. 148, 13–35.
Felden, J., Möller, L., Schindler, U., Huber, R., Schumacher, S., Koppe, R., Diepenbroek, M., Glöckner, F.O., 2023. PANGAEA - data publisher for Earth & environmental science. Sci. Data 10, 347.
Fletcher, W.J., Sánchez Goñi, M.F., 2008. Orbital- and sub-orbital-scale climate impacts on vegetation of the western Mediterranean basin over the last 48,000 yr. Quat. Res. 70, 451–464.
Fletcher, W.J., Sánchez Goñi, M.F., Allen, J.R.M., Cheddadi, R., Combourieu-Nebout, N., Huntley, B., Lawson, I., et al., 2010. Millennial-scale variability during the last glacial in vegetation records from Europe. Vegetation Response to Millennial-scale Variability during the Last Glacial 29, 2839–2864.
Fourcade, T., Goñi, M.F.S., Lahaye, C., Rossignol, L., Philippe, A., 2022a. Environmental changes in SW France during the Middle to Upper Paleolithic transition from the pollen analysis of an eastern North Atlantic deep-sea core. Quat. Res. 110, 147–164.
Fourcade, T., Lahaye, C., Goñi, M.F.S., 2022b. Cultural changes and adaptations to climatic and environmental changes of the last Neanderthals in southern France, Changements culturels et adaptations aux changements climatiques et environnementaux des derniers Néandertaliens dans le sud de la France. Université Michel de Montaigne - Bordeaux III.
Ganopolski, A., Rahmstorf, S., 2001. Rapid changes of glacial climate simulated in a coupled climate model. Nature 409, 153–158.
Gowan, E.J., Zhang, X., Khosravi, S., Rovere, A., Stocchi, P., Hughes, A.L.C., Gyllencreutz, R., et al., 2021. A new global ice sheet reconstruction for the past 80 000 years. Nat. Commun. 12, 1199.
Guiot, J., de Beaulieu, J.L., Cheddadi, R., David, F., Ponel, P., Reille, M., 1993. The climate in Western Europe during the last Glacial/Interglacial cycle derived from pollen and insect remains. 200 KA of global change 103, 73–93.
Heaton, T.J., Bard, E., Bronk Ramsey, C., Butzin, M., Hatté, C., Hughen, K.A., Köhler, P., Reimer, P.J., 2023a. A response to community questions on the MARINE20 radiocarbon age calibration curve: marine reservoir ages and the calibration of 14C samples from the oceans. Radiocarbon 65, 247–273.
Heaton, T.J., Butzin, M., Bard, E., Bronk Ramsey, C., Hughen, K.A., Köhler, P., Reimer, P. J., 2023b. Marine radiocarbon calibration in polar regions: a simple approximate approach using MARINE20. Radiocarbon 1–28.
Heinrich, H., 1988. Origin and consequences of cyclic ice rafting in the Northeast Atlantic Ocean during the past 130,000 years. Quat. Res. 29, 142–152.
Hemming, S.R., 2004. Heinrich events: massive late Pleistocene detritus layers of the North Atlantic and their global climate imprint. Rev. Geophys. 42.
Henry, L.G., McManus, J.F., Curry, W.B., Roberts, N.L., Piotrowski, A.M., Keigwin, L.D., 2016. North Atlantic ocean circulation and abrupt climate change during the last glaciation. Science 353, 470–474.
Heusser, L., Balsam, W.L., 1977. Pollen distribution in the northeast pacific ocean. Quat. Res. 7, 45–62.
Higham, T., Douka, K., Wood, R., Ramsey, C.B., Brock, F., Basell, L., Camps, M., et al., 2014. The timing and spatiotemporal patterning of Neanderthal disappearance. Nature 512, 306–309.
Higham, T., Frouin, M., Douka, K., Ronchitelli, A., Boscato, P., Benazzi, S., Crezzini, J., et al., 2024. Chronometric data and stratigraphic evidence support discontinuity between Neanderthals and early Homo sapiens in the Italian Peninsula. Nat. Commun. 15, 8016.
Hill, H.W., Flower, B.P., Quinn, T.M., Hollander, D.J., Guilderson, T.P., 2006. Laurentide Ice Sheet meltwater and abrupt climate change during the last glaciation. Paleoceanography 21.
Höbig, N., Weber, M.E., Kehl, M., Weniger, G.-C., Julià, R., Melles, M., Fülöp, R.-H., et al., 2012. Lake Banyoles (northeastern Spain): a Last Glacial to Holocene multi-proxy study with regard to environmental variability and human occupation. Quat. Int. 274, 205–218.
Hublin, J.-J., 2015. The modern human colonization of western Eurasia: when and where? Synchronising Environmental and Archaeological Records using Volcanic Ash Isochrons 118, 194–210.
Hussain, S.T., Floss, H., 2014. The role of river courses in organizing the cultural space of the Upper Paleolithic: examples from the Rhine, Rhône, Danube and Garonne. Modes de contacts et de déplacements au Paléolithique eurasiatique 307–320. ERAUL 140, ArchéoLogique 5, Liège, Luxembourg.
Huybers, P., Eisenman, I., 2006. Integrated summer insolation calculations. NOAA/NCDC Paleoclimatology Program data contribution 79.
Kageyama, M., Merkel, U., Otto-Bliesner, B., Prange, M., Abe-Ouchi, A., Lohmann, G., Ohgaito, R., et al., 2013. Climatic impacts of fresh water hosing under Last Glacial Maximum conditions: a multi-model study. Clim. Past 9, 935–953.
Kandel, A.W., Sommer, C., Kanaeva, Z., Bolus, M., Bruch, A.A., Groth, C., Haidle, M.N., et al., 2023. The ROCEEH Out of Africa Database (ROAD): a large-scale research database serves as an indispensable tool for human evolutionary studies. PLoS One 18, e0289513.
Kappenberg, A., Amelung, W., Conze, N., Sirocko, F., Lehndorff, E., 2021. Fire–vegetation relationships during the last glacial cycle in a low mountain range (Eifel, Germany). Palaeogeogr. Palaeoclimatol. Palaeoecol. 562, 110140.
Kapsch, M.-L., Graversen, R.G., Economou, T., Tjernström, M., 2014. The importance of spring atmospheric conditions for predictions of the Arctic summer sea ice extent. Geophys. Res. Lett. 41, 5288–5296.
Kim, J.-H., Schouten, S., Hopmans, E.C., Donner, B., Sinninghe Damsté, J.S., 2008. Global sediment core-top calibration of the TEX86 paleothermometer in the ocean. Geochem. Cosmochim. Acta 72, 1154–1173.
Klein, K., Weniger, G.-C., Ludwig, P., Stepanek, C., Zhang, X., Wegener, C., Shao, Y., 2023. Assessing climatic impact on transition from Neanderthal to anatomically modern human population on Iberian Peninsula: a macroscopic perspective. Science Bulletin.
Klein, R., 2000. Archeology and the evolution of human behavior. Evol. Anthropol. 9, 17–36.
Koreneva, E.V., 1966. Marine palynological researches in the U.S.S.R. Marine Palynology 4, 565–574.
van Kreveld, S., Sarnthein, M., Erlenkeuser, H., Grootes, P., Jung, S., Nadeau, M.J., Pflaumann, U., Voelker, A., 2000. Potential links between surging ice sheets, circulation changes, and the Dansgaard-Oeschger Cycles in the Irminger Sea, 60–18 Kyr. Paleoceanography 15, 425–442.
Kutzbach, J., Gallimore, R., Harrison, S., Behling, P., Selin, R., Laarif, F., 1998. Climate and biome simulations for the past 21,000 years. Quat. Sci. Rev. 17, 473–506.
Laepple, T., Lohmann, G., 2009. Seasonal cycle as template for climate variability on astronomical timescales. Paleoceanography 24.
Leroy, S.A.G., Arpe, K., Mikolajewicz, U., 2011. Vegetation context and climatic limits of the Early Pleistocene hominin dispersal in Europe. Early Human Evolution in the Western Palaearctic: Ecological Scenarios 30, 1448–1463.
Leroy, S.A.G., Giralt, S., Francus, P., Seret, G., 1996. The high sensitivity of the palynological record in the Vico maar lacustrine sequence (Latium, Italy) highlights the climatic gradient through Europe for the last 90 ka. Quat. Sci. Rev. 15, 189–201.
Li, C., Postl, A.K., Böhmer, T., Cao, X., Dolman, A.M., Herzschuh, U., 2022. Harmonized chronologies of a global late Quaternary pollen dataset (LegacyAge 1.0). Earth Syst. Sci. Data 14, 1331–1343.
Lippold, J., Grützner, J., Winter, D., Lahaye, Y., Mangini, A., Christl, M., 2009. Does sedimentary 231Pa/230Th from the Bermuda rise monitor past atlantic meridional overturning circulation? Geophys. Res. Lett. 36.
Lisiecki, L.E., Raymo, M.E., 2005. A Pliocene-Pleistocene stack of 57 globally distributed benthic delta O-18 records. Paleoceanography 20.
Liu, Z., Otto-Bliesner, B.L., He, F., Brady, E.C., Tomas, R., Clark, P.U., Carlson, A.E., et al., 2009. Transient simulation of last deglaciation with a new mechanism for bølling-allerød warming. Science 325, 310.
Lougheed, B.C., Obrochta, S.P., 2019. A rapid, deterministic age-depth modeling routine for geological sequences with inherent depth uncertainty. Paleoceanogr. Paleoclimatol. 34, 122–133.
Lougheed, B., Obrochta, S., 2016. MatCal: open source bayesian 14C age calibration in matlab. J. Open Res. Software 4.
Loutre, M.-F., Paillard, D., Vimeux, F., Cortijo, E., 2004. Does mean annual insolation have the potential to change the climate? Earth Planet Sci. Lett. 221, 1–14.
Ludwig, P., Shao, Y., Kehl, M., Weniger, G.-C., 2018. The Last Glacial Maximum and Heinrich event I on the Iberian Peninsula: a regional climate modelling study for understanding human settlement patterns. Global Planet. Change 140, 34–47.
Luetscher, M., Boch, R., Sodemann, H., Spötl, C., Cheng, H., Edwards, R.L., Frisia, S., et al., 2015. North atlantic storm track changes during the last glacial maximum recorded by alpine speleothems. Nat. Commun. 6, 6344.
Marciani, G., Carmignani, L., Djakovic, I., Roussel, M., Arrighi, S., Rossini, M., Boschin, F., et al., 2025. The uluzzian and châtelperronian: No technological affinity in a shared chronological framework. Journal of Paleolithic Archaeology 8, 3.
McManus, J.F., Francois, R., Gherardi, J.M., Keigwin, L.D., Brown-Leger, S., 2004. Collapse and rapid resumption of Atlantic meridional circulation linked to deglacial climate changes. Nature 428, 834–837.
Menviel, L., Timmermann, A., Friedrich, T., England, M.H., 2014. Hindcasting the continuum of Dansgaard–Oeschger variability: mechanisms, patterns and timing. Clim. Past 10, 63–77.
Monegato, G., Scardia, G., Hajdas, I., Rizzini, F., Piccin, A., 2017. The Alpine LGM in the boreal ice-sheets game. Sci. Rep. 7, 2078.
Moseley, G., Spötl, C., Brandstätter, S., Erhardt, T., Luetscher, M., Edwards, R., 2020. NALPS19: sub-orbital-scale climate variability recorded in northern Alpine speleothems during the last glacial period. Clim. Past 16, 29–50.
Movius, Jr H.L., 1969. The Châtelperronian in French archaeology: the evidence of Arcy-sur-Cure. Antiquity 43, 111–123.
Müller, U., Pross, J., Tzedakis, C., Gamble, C., Kotthoff, U., Schmiedl, G., Wulf, S., Christanis, K., 2011. The role of climate in the spread of modern humans into Europe. Quat. Sci. Rev. 30, 273–279.
Naughton, F., Sanchez Goñi, M.F., Desprat, S., Turon, J.-L., Duprat, J., Malaizé, B., Joli, C., et al., 2007. Present-day and past (last 25000 years) marine pollen signal off western Iberia. Mar. Micropaleontol. 62, 91–114.
Obreht, I., Hambach, U., Veres, D., Zeeden, C., Bösken, J., Stevens, T., Marković, S.B., et al., 2017a. Shift of large-scale atmospheric systems over Europe during late MIS 3 and implications for Modern Human dispersal. Sci. Rep. 7, 5848.
Obreht, I., Hambach, U., Veres, D., Zeeden, C., Bösken, J., Stevens, T., Marković, S.B., et al., 2017b. Shift of large-scale atmospheric systems over Europe during late MIS 3 and implications for Modern Human dispersal. Sci. Rep. 7, 5848.
Pedro, J.B., Andersson, C., Vettoretti, G., Voelker, A.H.L., Waelbroeck, C., Dokken, T.M., Jensen, M.F., et al., 2022. Dansgaard-Oeschger and Heinrich event temperature

anomalies in the North Atlantic set by sea ice, frontal position and thermocline structure. Quat. Sci. Rev. 289, 107599.
Pini, R., Furlanetto, G., Vallé, F., Badino, F., Wick, L., Anselmetti, F.S., Bertuletti, P., et al., 2022. Linking North Atlantic and Alpine Last Glacial Maximum climates via a high-resolution pollen-based subarctic forest steppe record. Quat. Sci. Rev. 294, 107759.
Prentice, I.C., Cramer, W., Harrison, S.P., Leemans, R., Monserud, R.A., Solomon, A.M., 1992. Special paper: a global biome model based on plant physiology and dominance, soil properties and climate. J. Biogeogr. 19, 117–134.
Rasmussen, T.L., Thomsen, E., Moros, M., 2016. North Atlantic warming during Dansgaard-Oeschger events synchronous with Antarctic warming and out-of-phase with Greenland climate. Sci. Rep. 6, 20535.
Rathmann, H., Vizzari, M.T., Beier, J., Bailey, S.E., Ghirotto, S., Harvati, K., 2024. Human population dynamics in Upper Paleolithic Europe inferred from fossil dental phenotypes. Sci. Adv. 10, eadn8129.
Reimer, P.J., Austin, W.E.N., Bard, E., Bayliss, A., Blackwell, P.G., Bronk Ramsey, C., Butzin, M., et al., 2020. The IntCal20 northern hemisphere radiocarbon age calibration curve (0–55 cal kBP). Radiocarbon 62, 725–757.
Reimer, P.J., Reimer, R.W., 2001. A marine reservoir correction database and on-line interface. Radiocarbon 43, 461–463.
Roebroeks, W., 2014. Terra incognita: the Palaeolithic record of northwest Europe and the information potential of the southern North Sea. Netherlands Journal of Geosciences - Geologie en Mijnbouw 93, 43–53.
Rohling, E.J., Grant, K., Bolshaw, M., Roberts, A.P., Siddall, M., Hemleben, Ch, Kucera, M., 2009. Antarctic temperature and global sea level closely coupled over the past five glacial cycles. Nat. Geosci. 2, 500–504.
Rohling, E.J., Grant, K., Hemleben, C., Kucera, M., Roberts, A.P., Schmeltzer, I., Schulz, H., et al., 2008. New constraints on the timing of sea level fluctuations during early to middle marine isotope stage 3. Paleoceanography 23.
Sanchez Goñi, M., Desprat, S., Fletcher, W., Morales-Molino, C., Naughton, F., Oliveira, D., Urrego, D., Zorzi, C., 2018. Pollen from the deep-sea: a breakthrough in the mystery of the ice ages. Front. Plant Sci. 9.
Sánchez Goñi, M.F., 2020. Regional impacts of climate change and its relevance to human evolution. Evolutionary Human Sciences 2, e55.
Sánchez Goñi, M.F., Desprat, S., Daniau, A.-L., Bassinot, F.C., Polanco-Martínez, J.M., Harrison, S.P., Allen, J.R.M., et al., 2017. The ACER pollen and charcoal database: a global resource to document vegetation and fire response to abrupt climate changes during the last glacial period. Earth Syst. Sci. Data 9, 679–695.
Sánchez Goñi, M.F., Eynaud, F., Turon, J.L., Shackleton, N.J., 1999. High resolution palynological record off the Iberian margin: direct land-sea correlation for the Last Interglacial complex. Earth Planet Sci. Lett. 171, 123–137.
Sánchez Goñi, M.F., Landais, A., Fletcher, W.J., Naughton, F., Desprat, S., Duprat, J., 2008. Contrasting impacts of Dansgaard–Oeschger events over a western European latitudinal transect modulated by orbital parameters. Quat. Sci. Rev. 27, 1136–1151.
Schmidt, I., Gehlen, B., Winkler, K., Arrizabalaga, A., Arts, N., Bicho, N., Crombé, P., et al., 2024. Demographic responses to climatic changes during the final palaeolithic in Europe. bioRxiv: 2024.09.11.612499.
Shackleton, N.J., Hall, M.A., Vincent, E., 2000. Phase relationships between millennial-scale events 64,000–24,000 years ago. Paleoceanography 15, 565–569.
Shao, Y., Limberg, H., Klein, K., Wegener, C., Schmidt, I., Weniger, G.-C., Hense, A., Rostami, M., 2021. Human-existence probability of the Aurignacian techno-complex under extreme climate conditions. Quat. Sci. Rev. 263, 106995.
Shao, Y., Wegener, C., Klein, K., Schmidt, I., Weniger, G.-C., 2024. Reconstruction of human dispersal during Aurignacian on pan-European scale. Nat. Commun. 15, 7406.
Silvestrini, S., Romandini, M., Marciani, G., Arrighi, S., Carrera, L., Fiorini, A., López-García, J., et al., 2021. Integrated multidisciplinary ecological analysis from the Uluzzian settlement at the Uluzzo C Rock Shelter, south-eastern Italy. J. Quat. Sci. 37.
Sirocko, F., Knapp, H., Dreher, F., Förster, M.W., Albert, J., Brunck, H., Veres, D., et al., 2016. The ELSA-vegetation-stack: reconstruction of landscape evolution zones (LEZ) from laminated eifel maar sediments of the last 60,000years. Global Planet. Change 142, 108–135.
Stanley, E.A., 1966. The application of palynology to oceanology with reference to the northwestern Atlantic. Deep Sea Res. Oceanogr. Abstr. 13, 921–939.
Stewart, J.R., Stringer, C.B., 2012. Human evolution out of Africa: the role of refugia and climate change. Science 335, 1317–1321.
Stott, L., Timmermann, A., Thunell, R., 2007. Southern hemisphere and deep-sea warming led deglacial atmospheric CO2 rise and tropical warming. Science 318, 435–438.
Sung, M.-K., An, S.-I., Shin, J., Park, J.-H., Yang, Y.-M., Kim, H.-J., Chang, M., 2023. Ocean fronts as decadal thermostats modulating continental warming hiatus. Nat. Commun. 14, 7777.
Svensson, A., Andersen, K.K., Bigler, M., Clausen, H.B., Dahl-Jensen, D., Davies, S.M., Johnsen, S.J., et al., 2008. A 60 000 year Greenland stratigraphic ice core chronology. Clim. Past 4, 47–57.
Svensson, A., Andersen, K.K., Bigler, M., Clausen, H.B., Dahl-Jensen, D., Davies, S.M., Johnsen, S.J., et al., 2006. The Greenland Ice Core Chronology 2005, 15–42ka. Part 2: comparison to other records. Critical Quaternary Stratigraphy 25, 3258–3267.
Tierney, J.E., Tingley, M.P., 2014. A Bayesian, spatially-varying calibration model for the TEX86 proxy. Geochem. Cosmochim. Acta 127, 83–106.
Tierney, J.E., Tingley, M.P., 2018. BAYSPLINE: a new calibration for the alkenone paleothermometer. Paleoceanogr. Paleoclimatol. 33, 281–301.
Timmermann, A., Raia, P., Mondanaro, A., Zollikofer, C.P.E., Ponce de León, M., Zeller, E., Yun, K.-S., 2024. Past climate change effects on human evolution. Nat. Rev. Earth Environ. 5, 701–716.
Tomasso, A., Porraz, G., 2016. Hunter-gatherers' mobility and embedded raw material procurement strategies: a critical view from the Mediterranean Upper Paleolithic. Evol. Anthropol. Issues News Rev. 25, 164–174.
Veres, D., Bazin, L., Landais, A., Toyé Mahamadou Kele, H., Lemieux-Dudon, B., Parrenin, F., Martinerie, P., et al., 2013. The Antarctic ice core chronology (AICC2012): an optimized multi-parameter and multi-site dating approach for the last 120 thousand years. Clim. Past 9, 1733–1748.
Waelbroeck, C., Lougheed, B.C., Vazquez Riveiros, N., Missiaen, L., Pedro, J., Dokken, T., Hajdas, I., et al., 2019. Consistently dated Atlantic sediment cores over the last 40 thousand years. Sci. Data 6, 165.
Wegwerth, A., Ganopolski, A., Ménot, G., Kaiser, J., Dellwig, O., Bard, E., Lamy, F., Arz, H., 2015. Black Sea temperature response to glacial millennial-scale climate variability. Geophys. Res. Lett. 42, 2015GL065499.
Williams, J.W., Grimm, E.C., Blois, J.L., Charles, D.F., Davis, E.B., Goring, S.J., Graham, R.W., et al., 2018. The Neotoma Paleoecology Database, a multiproxy, international, community-curated data resource. Quat. Res. 89, 156–177.
Wolff, E.W., Chappellaz, J., Blunier, T., Rasmussen, S., Svensson, A., 2010. Millennial-scale variability during the last glacial: the ice core record. Quat. Sci. Rev. 29.
Xu, G., Broadman, E., Dorado-Liñán, I., Klippel, L., Meko, M., Büntgen, U., De Mil, T., et al., 2024. Jet stream controls on European climate and agriculture since 1300 ce. Nature.
Zheng, P., Pedro, J.B., Jochum, M., Rasmussen, S.O., Lai, Z., 2021. Different trends in antarctic temperature and atmospheric CO2 during the last glacial. Geophys. Res. Lett. 48, e2021GL093868.
Zilhão, J., d'Errico, F., Banks, W.E., Teyssandier, N., 2024. A data-driven paradigm shift for the middle-to-upper palaeolithic transition and the neandertal debate. Quaternary Environments and Humans 2, 100037.